1-2006

Fabrication-tolerant active-passive integration scheme for vertically-coupled microring resonators

Chyng Wen TEE
Singapore Management University, cwtee@smu.edu.sg

KA Williams

RV Penty

IH White

Citation

TEE, Chyng Wen; Williams, KA; Penty, RV; and White, IH. Fabrication-tolerant active-passive integration scheme for vertically-coupled microring resonators. (2006). *IEEE Journal of Selected Topics in Quantum Electronic*. 12, (1), 108-116. Research Collection Lee Kong Chian School Of Business.
Available at: https://ink.library.smu.edu.sg/lkcsb_research/3337

Published in IEEE Journal of Selected Topics in Quantum Electronics, 2006 January, Volume 12, Issue 1, Pages 108-116
https://doi.org/10.1109/JSTQE.2005.862947

Fabrication-Tolerant Active–Passive Integration Scheme for Vertically Coupled Microring Resonator

Chyng Wen Tee, *Student Member, IEEE*, Kevin A. Williams, *Member, IEEE*, Richard V. Penty, *Member, IEEE*, and Ian H. White, *Fellow, IEEE*

***Abstract*—The large-scale photonic integration of microring resonators in three dimensions made possible by recent developments in vertical coupling and wafer bonding technology is shown to be sensitive to lateral mask misalignment for the ring and bus waveguides introduced during the fabrication process. For a typical 20-μm radius, vertically coupled microring calculations reveal a linear relationship between deviation in the coupling coefficient and lateral misalignment. A coupling coefficient reduction of 50% is predicted for a lateral misalignment of 0.3 μm, which is typical for an alignment accuracy limited by the current state-of-the-art mask alignment process. The use of a wide multimode bus waveguide is proposed to ameliorate this alignment sensitivity. The mode-expanded bus waveguide, together with its physically wider structure, reduces the dependence of modal overlap and coupling length on precise alignment, resulting in significantly relaxed fabrication tolerance. Deviation of coupling coefficient decreases by an order of magnitude for the new ring coupler geometry, where a sole reduction of 5% is obtained for the same amount of misalignment. The implications of the proposed structure are subsequently investigated for microring laser performance. The differential slope efficiency is shown to be at least five times less sensitive to lateral misalignment for the proposed structure within a small misalignment regime. This readily adaptable coupler geometry based on existing vertical coupling architectures is transferable to any fabrication scheme with multiple waveguide layers coupled vertically, and is of particular importance to microring resonators with small radii.**

***Index Terms*—Electromagnetic propagation, fiber coupling, large-scale integration, multimode waveguides, optical coupling, optical diffraction, optical fiber coupling, optical planar waveguides, optical resonators, semiconductor device fabrication, semiconductor device modeling, semiconductor microring, waveguide couplers.**

I. Introduction

THE development of the optical communication network and the implementation of dense wavelength-division-multiplexing (DWDM) fiber-optic communication systems have driven the need to realize large scale photonic integrated circuits with high speed performance. Eventually, advances in semiconductor fabrication technologies are expected to enable the monolithic integration of several photonic components within important optical modules such as transmitter/receivers, optical switch fabrics, multiplexer/demultiplexers, wavelength converters, and optical logic gates into a single optoelectronic chip. In contrast to conventional manual assembly of individual optical modules from discrete components, integrated photonic components allow substantial improvements in size, robustness, and power consumption of the implemented device. To this end, however, the integration of optical waveguide interconnects and active–passive waveguides constitutes a major technological obstacle, limiting the manufacturability, complexity, and scalability of future photonic integration.

Microring resonators are a highly attractive and increasingly viable candidates for photonic integration [1], [2] due to the wide range of applications achievable via their attractive wavelength selectivity and compact feature size. They are functionally analogous to Fabry–Perot resonators, without, however, the need to form edge mirrors by cleaving or high performance etching. As such, they are suitable for use as optical cavities for applications as lasers, optical filters, channel add-drop multiplexer/demultiplexers, active optical switches, and optical logic elements. A microring device generally makes use of straight bus waveguides to couple light in and out of the ring resonator, and is therefore primarily characterized by its ring radius and coupler geometry. The ring radius is specified by the required performance of the device; the coupler geometry, on the other hand, falls into two main fabrication process-defined categories: laterally coupled and vertically coupled. Laterally coupled microring structures were the first to be realized. In this geometry, the ring and bus waveguides lie in the same epitaxial plane. For components formed using the III–V material systems, epilayers are grown by molecular beam epitaxy on an InP or GaAs substrate. The features of the microring and bus waveguides are typically defined by electron beam lithography. A combination of reactive-ion etching and chemical-assisted ion beam etching is then employed to transfer the pattern onto the epilayer [3], [4]. The drawbacks of this approach are twofold. Firstly, the coupling gap between the microring and bus waveguides is defined by electron beam lithography and the subsequent processing steps, which have a process-dependent variability, making it difficult to achieve reproducible device performance. Secondly, the fact that the microring and bus waveguides lie in the same epitaxy plane places a constraint on the material processing flexibility which, for instance, prevents active–passive integration. For this reason, vertically coupled structures had been explored rigorously over the past decades [5]–[8], exploiting the freedom to tailor the epitaxial configuration for the active and passive layers separately.

Manuscript received December 31, 2004; revised November 7, 2005. This work was supported in part by the European Community through the research project WAPITI (Wafer-bonding and Active Passive Integration Technology and Implementation, FP6-2003-IST-2-004073).

The authors are with the Center for Photonic Systems, Engineering Department, Cambridge University, Cambridge CB3 0FD, U.K. (e-mail: cwt23@cam.ac.uk).

Digital Object Identifier 10.1109/JSTQE.2005.862947

Until recently, both vertically coupled and laterally coupled architectures are restricted by the single-sided fabrication scheme, where lossy ridge or rib waveguides are used to provide optical confinement. Recent progress in wafer-bonding technology has enabled the capability to process both side of a single wafer, thus yielding waveguides integrated in three dimensions [3], [4]. The limitation in previous ring coupler geometry can therefore be overcome by the introduction of a three-dimensional (3-D) vertically coupled structure, where the independently optimized microring and bus waveguides are implemented on different epilayers and are coupled to each other vertically through an epitaxially grown separation layer. The fabrication process of vertically coupled microring devices can be summarized as follows: the bus waveguides are first fabricated by epitaxial growth and selective etching. An insulating cladding layer is then applied to the structure prior to wafer bonding to another substrate. The sample is then inverted, and the substrate of the original wafer is removed by etching. Finally, the microring waveguide is patterned and fabricated by standard lithography and etching subsequent to mask alignment [3], [4].

To date, a wide range of applications have been demonstrated in microring resonators. Laterally coupled semiconductor ring lasers [9], [10] with ring radii in the range of $\sim$500 μm have been fabricated, showing the feasibility of a mirror-free semiconductor light source suitable for photonic integration. Further reduction in the ring laser's dimensions have, however, been hampered by processing difficulties such as sidewall-roughness-induced scattering loss in the ridge ring waveguide, which restricts the bending radius. The circulating optical path can be used as either laterally-or vertically coupled high order filters [11]–[14], or WDM channel add-drop filters [15]–[18] with microrings cascaded in series or parallel. Both dielectric and semiconductor rings filters have been realized. In contrast to weakly-guided laterally coupled rings where a typical radius ranges from 300–700 μm [11], [16], vertically coupled architectures are capable of realizing smaller ring radii at the range of 10–20 μm due to the better optical confinement achievable, thus benefiting from a wider free spectral range for minimal signal crosstalk [12]–[14], [18]. Active switching of the optical signals with applied bias has also been achieved using laterally- [19] or vertically coupled [20] structures. Furthermore, the signal intensity within the microring can be substantially enhanced internally when the resonance condition is satisfied, giving rise to various nonlinear optical phenomena. Wavelength conversion by means of four-wave mixing [21] and optical logic generated via two-photon absorption [22] has recently been demonstrated. Clearly, the drive for large scale photonic integration suggests that vertical coupling is more favorable due to the ease of miniaturization. Moreover, compact 3-D active–passive integration is also more feasible with the schemes such as the two-sided wafer processing method made possible by wafer-bonding technology.

Vertically coupled microring structures have the potential for higher manufacturing reproducibility and yield. The coupling gap between the microring and bus waveguide is epitaxially grown in the vertical coupling scheme, making it more controllable than the lateral coupling scheme where the dimension of the gap is limited by the accuracy of the etching process. In addition, the high refractive-index semiconductor separation layer in the vertically coupled structure also relaxes the fabrication tolerance compared to low index separation materials such as air, passivation layers, or metallization employed in laterally coupled structures. The fact that the two waveguides reside at different epilayers also makes it possible to optimize their corresponding dimensions and structures independently. Therefore, vertical coupling architecture reduces the main fabrication imperfections to one single issue-mask alignment between the microring and bus waveguides. The state-of-the-art wafer bonding technique currently leads to an alignment accuracy of ± 0.3 μm [27]. This work addresses this limit of integration, and looks at potential extensions that can be readily adapted to improve the fabrication tolerance of the state-of-the-art 3-D fabrication techniques.

In this paper, a 3-D mode propagation solver is implemented to investigate the influence of lateral misalignment on the coupling of modes between microring and bus waveguides of equal width. The feasibility of improving the alignment tolerance by doubling the width of the bus waveguide is then studied. The matching of this multimode waveguide to a single-mode waveguide for connection to other integrated photonic components can be achieved by tapering the width down to cutoff for the higher order modes. Lateral mode matching to single-mode fiber can also be realized by implementing a double taper configuration that reduces lateral modal diffraction. This paper is organized as follows. In Section II, the structure of a vertically coupled microring resonator is presented. An introduction to the simulation model is given in Section III. Numerical results of the waveguiding analysis by means of mode propagation solver are elaborated upon in Section IV, along with implications for lasers fabricated using the relaxed tolerance scheme. Finally, a summary and our conclusions on optimum design are given in Section V.

II. Device Structure

The schematic of a vertically coupled microring device considered in our analysis is shown in Fig. 1(a). The ring waveguide, which is sandwiched between two InP cladding layers, has a bandgap of $Q_{\mathrm{Ring}} = 1290$ nm. The ring radius is perfectly circular and has a radius of curvature of 20 μm. A buried heterostructure bus waveguide, with a bandgap identical to that of the ring waveguide, is located underneath the ring. This bus waveguide is cladded by silica, which serves both to improve modal confinement and facilitate wafer bonding for structural support. A detailed plan and cross-sectional view is also presented in Fig. 1(b). Lateral misalignment is defined as the distance measured between the center of the ring and the bus waveguide. The coupling coefficient between the active-ring and passive-bus waveguide is, therefore, a function of both waveguide separation and lateral misalignment.

The waveguide separation between the microring and bus waveguide is made up of the waveguide cladding layer and the mid-layer. The thickness of this mid-layer is dependent on the etch depth during the fabrication process of the top microring waveguide, as shown in Fig. 1(b). Typically, a thin layer of the

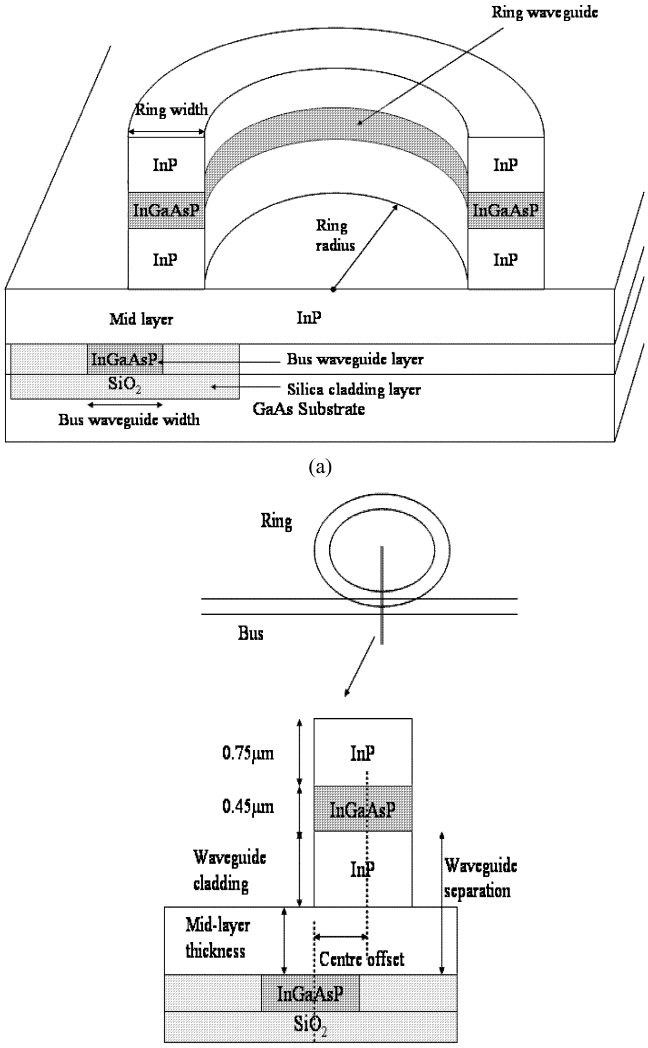

Fig. 1. (a) Schematic of vertically coupled microring device. (b) Plan and cross-sectional view of the device; waveguide parameter used in the paper is specified.

original InP waveguide separation layer is left intact during the etching process, effectively splitting it into the two functional layers stated previously: a rib waveguide for the active microring layer for tight optical confinement, and a ridge waveguide for the passive bus layer for low loss operation. While it is clear that, for a given microring-bus separation, a smaller mid-layer thickness provides better modal confinement within the ring waveguide, resulting in a reduced optical attenuation due to bending loss, it has been shown previously that leaving a thin mid-layer has the effect of improving coupling efficiency and providing mechanical support to the microring waveguide layer [27].

III. Numerical Technique

A 3-D eigenmode expansion (EME) method [31] is used to model the vertically coupled microring device. The model is very computationally efficient for analyzing waveguide structures with optical field confined along the transverse (x, y) direction, while the waveguide itself is slowly-varying along the propagation (z) direction. This particular waveguide geometry allows one to separate the solution of the Helmholtz equation into a complete basis set of two-dimensional (2-D) eigenmodes and one propagation direction with a simple harmonic dependence as follows [32]:

$$\Psi(x, y, z) = \sum_{k=1}^{N} \{A_k \exp(j\beta_k z) \pm B_k \exp(-j\beta_k z)\} \psi_k(x, y) \tag{1}$$

where Ψ and ψ are the electric or magnetic field amplitude and mode profiles, respectively, A and B are the forward and backward propagating field amplitude, β is the propagation constant, and k signifies the eigenmodes included in the analysis. While the complete basis set of eigenmodes consists of an infinite number of modes, in general, accounting for the guided-modes within the waveguide will be sufficient to accurately compute waveguiding problems with reasonably low numerical error [32]. A given waveguide structure is separated longitudinally into an array of waveguide sections, each of which is written as a linear combination of 2-D eigenmodes calculated by a vectorial film mode-matching method [33]. Field amplitudes in each waveguide section are then determined by evaluating the scattering matrices between adjacent waveguides, which are obtained from mode overlap integrals of eigenmodes in neighboring waveguides. Once these parameters are computed, field propagation across the entire waveguide can then be simulated.

The waveguide structure described in Section II is investigated under the preceding algorithm [31]. As this work focuses on the mode coupling between the ring and bus waveguide, the microring dimension is designed to ensure single-mode ring performance, and only half of the ring circumference where the mid-point overlaps with the bus waveguide is considered in the analysis. The coupling coefficient (κ), defined as the fraction of power coupled to an adjacent waveguide at the coupling section, is evaluated by injecting a fundamental transverse magnetic mode (TM) at the microring as input, and computing the fraction of optical power output from the bus waveguide. Note that although the TM mode is considered in the simulation, mode coupling in a vertically coupled structure is polarization insensitive [3], [4]; therefore, the results obtained are general and can be applied equally well to the TE mode.

IV. Simulations

In the following, the coupling of modes between the microring and bus waveguide is analyzed. Initial studies concentrated on the alignment sensitivity of a conventional vertically coupled microring architecture, where both microring and bus are single-moded waveguides with identical width. The feasibility of employing a multimode bus as an alternative approach to reduce the sensitivity of the mode coupling coefficient to alignment offset is subsequently proposed. A double taper configuration for the bus waveguide is also introduced to discriminate against higher order modes, and enhance mode matching to single mode fiber for better butt-coupling efficiency. A comparison for laser designs

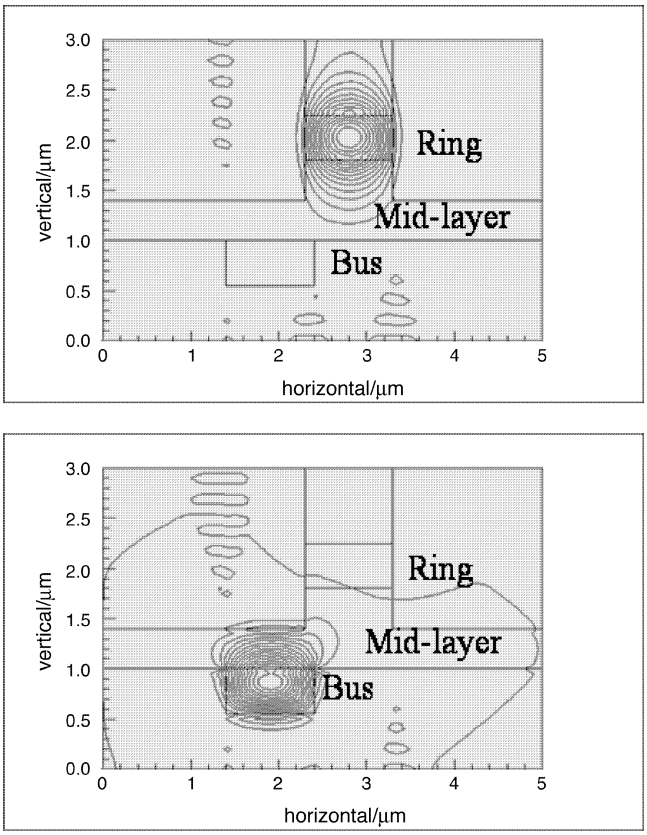

Fig. 2. Field contour plot of the transverse magnetic mode within the microring and bus waveguide. The two waveguides are inherently single-moded.

based on the conventional and the proposed structures is also presented to highlight the implications on device fabrication.

A. Conventional Design-Single-Moded Ring and Bus Waveguide

Conventional vertically coupled microring architectures employ narrow width ring and bus waveguides to ensure single-mode performance. The width of ring and bus waveguide is set to 1 μm in the calculation, which is typical of published work. Fig. 2 shows the field contour plot of the fundamental transverse magnetic mode within the two waveguides, which are inherently single-moded.

The vertical separation between the ring and bus waveguide is epitaxially controlled, and achieves a high level of precision. The variation in offsets between the center points of the microring and bus waveguide due to lateral misalignment during the fabrication process thereby constitutes a major fabrication issue in the vertically coupled architecture. In Fig. 3, the dependence of power coupling coefficient on lateral alignment of the microring and bus waveguide is plotted with a range of midlayer thicknesses. The waveguide separation is set to 0.8 μm, and the waveguide cladding and midlayer thickness combinations are varied in the three curves. While positive offsets whereby the ring moves away from the bus are considered in Fig. 3, it is noted that negative offsets of comparable magnitude have a significantly weaker effect. The results of the calculation show clearly

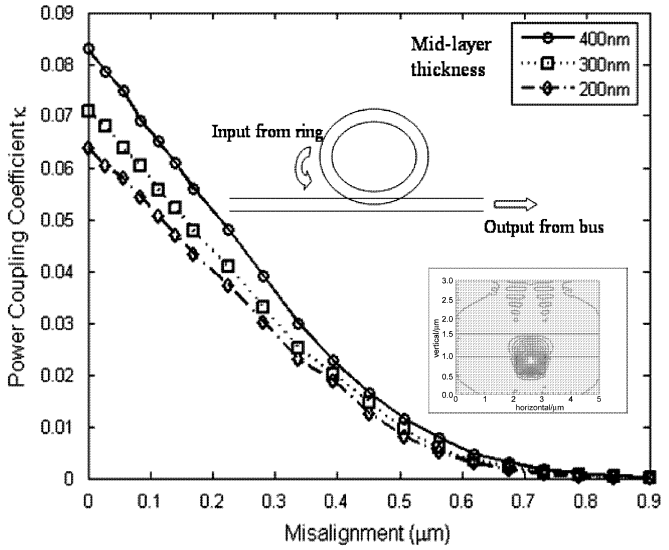

Fig. 3. Dependence of power coupling coefficient on lateral misalignment of microring and single-mode bus waveguide. There is a linear relationship between the rolloff in the coupling coefficient and lateral misalignment within a small offset regime (± 0.3 μm).

that a slight lateral misalignment leads to a drastic deviation from the optimum coupling coefficient. A linear dependence of coupling coefficient as a function of misalignment is observed within the small lateral misalignment regime (<0.5 μm). A lateral offset of ~ 0.3 μm corresponds to a 50% reduction in the coupling coefficient. The influence of the midlayer thickness on the coupling of modes between the two waveguides is also shown in the figure. For a given waveguide separation, a thicker midlayer thickness has the advantage of enhanced mode coupling due to the additional high-index waveguiding region for mode-coupling between the microring and bus waveguide to take place. However, a higher bending loss from the ring waveguide should be anticipated, since the smaller waveguide cladding layer inevitably reduces modal confinement within the ring. It has been shown theoretically and experimentally that to avoid bending loss in the ring waveguide, a typical midlayer thickness of smaller than 400 nm is required [4].

The computational results of the 3-D mode propagation solver can be readily explained within the framework of coupled-mode theory [15], which predicts that the coupling coefficient between two weakly-coupled waveguides in close proximity is dependent on the corresponding mode overlap profile within the two waveguides, as well as the length of the overlap region [15]

$$\kappa = -j\frac{\omega\varepsilon_0}{4}\int_{L_c} dz \int\int dxdy\left(n^2 - n_B^2\right)\psi_1\psi_2 \exp(-j\beta z) \tag{2}$$

where ω is the angular frequency of the guided-mode, ε_0 is the material's permittivity, L_c is the coupling length, n_B is the refractive index of the waveguide separation layer, and ψ_1 and ψ_2 are the mode profile within the ring and bus waveguide, respectively. Clearly, lateral misalignment leads to a reduction in the coupling coefficient as a consequence of the decrease

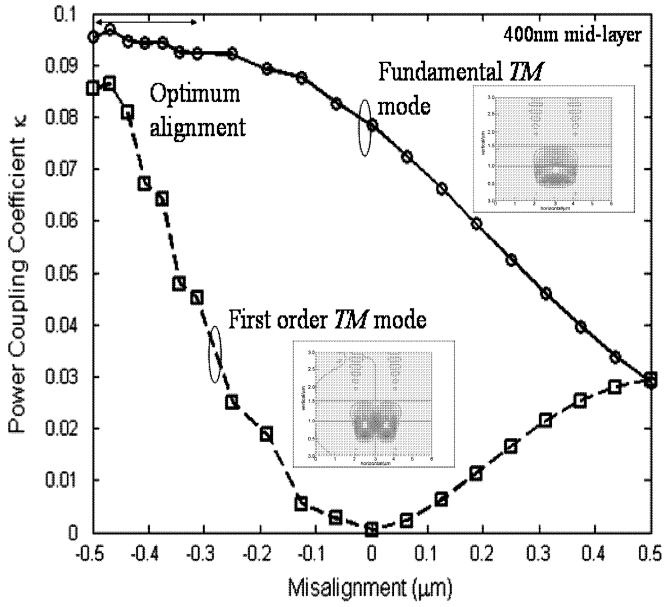

Fig. 4. Dependence of power coupling coefficient on lateral misalignment of microring and multimode bus waveguide. Although a higher order mode will be excited, the wider mode profile supported by the multimode bus waveguide significantly reduces the sensitivity of the coupling coefficient to misalignment.

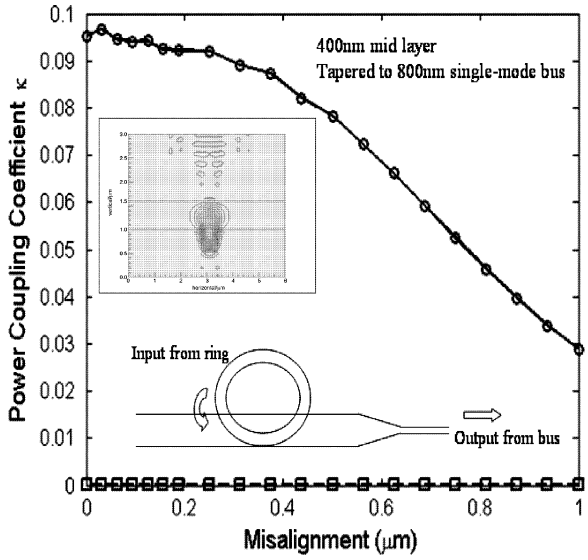

Fig. 5. Power coupling coefficient to multimode bus waveguide with taper architecture employed to provide higher order mode filtering within the multimode bus waveguide.

in mode overlap product $(\psi_1\psi_2)$ and length of the overlap region (L_c).

B. Relaxed Fabrication Tolerance Design

In Section IV-A, reduced modal overlap and effective coupling length are identified as the principle mechanisms behind the reduction of coupling coefficient with increasing lateral bus/ring misalignment. This suggests that deviation of the coupling coefficient from the designed value can be minimized by reducing the dependence of the two parameters on lateral misalignment, thereby relaxing the fabrication tolerance of the design. We propose the use of a mode-expanded wide multimode bus waveguide to ameliorate this coupling effect. A wider waveguide supports a wider mode profile, which reduces the sensitivity of effective coupling length and mode overlap integral to lateral alignment. This is consistent with the framework of coupled-mode theory as defined in (2), which indicates that a reduced coupling sensitivity on lateral misalignment can be achieved by applying a mode-expanded bus waveguide with a wider width.

The coupling coefficient is calculated using an approach similar to the approach outlined in Section III. Due to the inherent multimode nature of the bus waveguide design, two modes are excited at the coupling region. Fig. 4 plots the dependence of power coupling coefficient from the ring to the fundamental and first order TM mode in the multimode bus waveguide at various midlayer thicknesses. The field contour plots of the two modes are shown in the inset of the figure. A midlayer thickness of 400 nm is used in the calculation. From the figure, it is observed that the coupling coefficient of the fundamental mode (solid line) is maximized at a center offset value of -0.5 μm, where the waveguide overlap region is the largest. The roll-off of coupling coefficient is much slower than that of the single-mode bus waveguide, as depicted in Fig. 3. The coupling coefficient to the first order TM mode (dotted line) is also shown in the figure. Enhanced coupling to the first order mode occurs at a lateral misalignment of -0.5 μm and $+0.5$ μm, where the modal overlap is significant.

Although perfectly aligning the center of the ring and bus waveguides will result in an improved coupling sensitivity and minimal excitation of the higher order mode, it is observed that the coupling coefficient for the fundamental mode remains unchanged within the regime of small lateral misalignment with a center offset of -0.5 μm, as indicated in Fig. 4. This is because while lateral misalignment decreases the waveguide overlap region, the mode overlap integral actually increases, canceling the effect of the misalignment on the coupling coefficient. When the microring and bus waveguide is aligned to this optimum offset value, the deviation of coupling coefficient from the designated value remains smaller than 5% for a lateral misalignment of 0.3 μm, showing that fabrication tolerance can be significantly relaxed by employing a mode expanded bus waveguide.

C. Double Taper Configuration

It is desirable to achieve mode-matching to a single-mode bus waveguide for connection to other integrated photonic components, or for enhanced coupling efficiency between a bus waveguide with slab geometry and a single-mode fiber with cylindrical geometry. The aim of this section is to analyze and discuss the feasibility of adapting a simple taper architecture to achieve these two goals.

Adiabatic tapers within the bus waveguide can be used to introduce intermodal discrimination to the guided modes. By tapering the width of the wide multimode bus to below the cut-off value of the higher order modes, efficient mode filtering can be achieved. Fig. 5 plots the power coupling efficiency with the

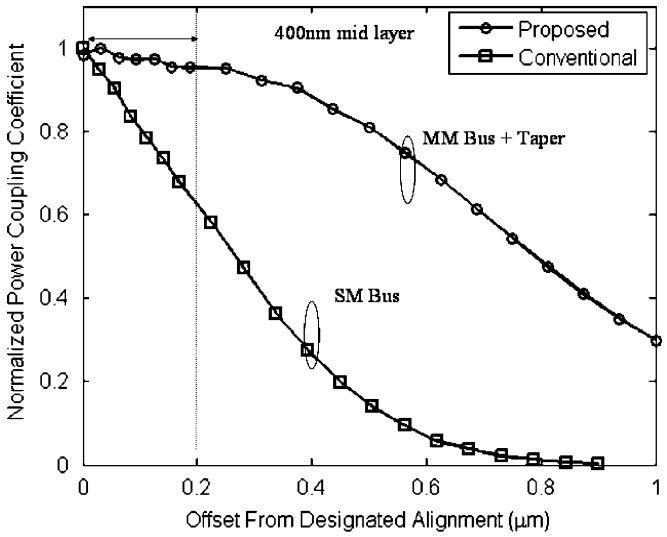

Fig. 6. Graphical comparisons between conventional and proposed design. Within the regime of small offset (± 0.3 μm), deviation of the coupling coefficient from the proposed design is minimal ($\sim 5\%$), whereas in the conventional design the deviation is as high as 50%.

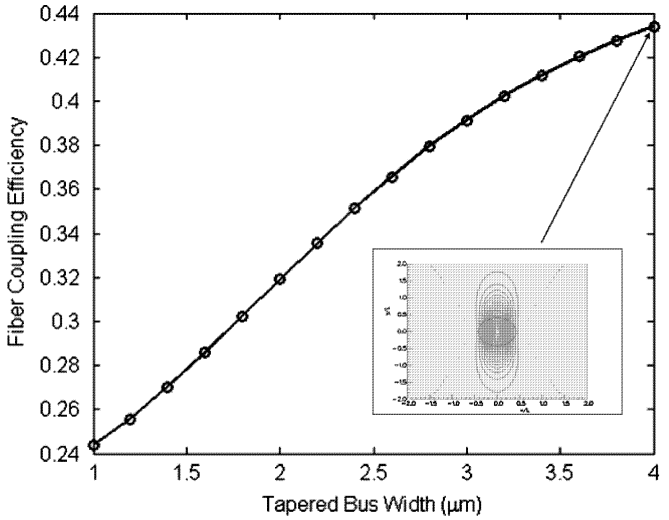

Fig. 7. Coupling efficiency of different bus waveguide widths to single mode fiber at a distance of 15 μm and a core diameter of 12.5 μm. To ensure efficient butt-coupling to fiber, an in-and-out taper configuration is useful in reducing lateral diffraction, resulting in enhanced spot-size matching to the fiber geometry in one dimension, as shown in the inset of the figure.

existence of a tapered bus section that reduces the width of the bus to 0.8 μm beyond the waveguide overlap region where mode coupling takes place. Due to the presence of the low refractive index silica cladding around the bus waveguide, a tapering section with a length as small as 200 μm is sufficient to ensure adiabatic performance. The field contour plot of the fundamental mode within the tapered single-mode bus waveguide is also shown in the inset of the figure. The calculation results show clearly that the optical power coupled to the higher order mode is filtered after the taper section, while coupling to the fundamental mode is unaffected. A graphical comparison between the conventional and proposed designs is plotted in Fig. 6. Although both designs operate in the single-mode regime, for a given lateral misalignment from designated alignment, the deviation of coupling coefficient is significantly smaller for the proposed design.

Input–output coupling losses from the narrow bus waveguide to the single-mode fiber can increase to up to 30 dB [34] as a result of spot-size mismatch between the two waveguides. Optical output from the narrow bus waveguide undergoes a large amount of diffraction. However, enhanced fiber coupling efficiency can be obtained by expanding the fundamental mode profile after the higher order mode filtering section. This wide mode profile leads to reduced lateral diffraction, enhancing mode matching to the single mode fiber. Therefore, a double taper configuration that tapers the bus waveguide in-and-out is efficient for mode filtering and fiber coupling efficiency. Fig. 7 shows a plot of the fiber coupling efficiency versus tapered bus width. The distance between the bus waveguide and fiber is set to 15 μm in the calculation. The far field contour plot and its corresponding overlap profile with the single-mode fiber (dark circle) are also plotted in the inset of the figure. Spot-size matching along the horizontal direction is achieved by a wide taper bus. The calculations presented in this section provide a firm theoretical justification of

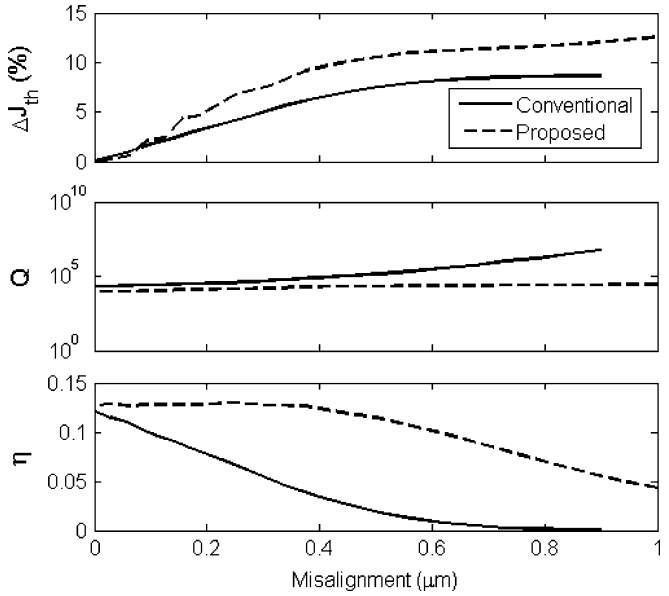

Fig. 8. Dependence of threshold current density deviation, quality factor, and differential slope efficiency of vertically coupled microring laser on lateral misalignment.

the taper configuration that had been experimentally evaluated for enhanced fiber coupling efficiency in [26], [27].

D. Device Applications-Microring Lasers

A microring device is characterized by its ring radius, epitaxial layer, coupling coefficient and cavity loss (due to side-wall roughness and scattering) [23]–[29]. For a given design, the most important parameter that can severely impact the performance of the device is the coupling coefficient [3], [4], which specifies the optical power coupling efficiency between the ring and bus waveguide. Previous sections have explored a readily adaptable coupler geometry to ameliorate this issue. It is

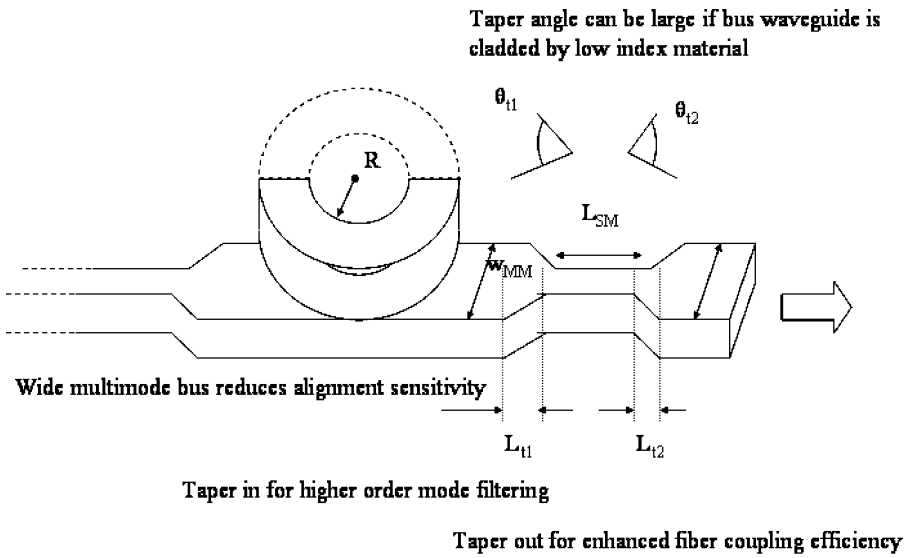

Fig. 9. Schematic of proposed vertically coupled microring architecture. Wide multimode bus reduces the power coupling sensitivity to lateral misalignment. Double taper configuration provides higher order mode filtering and improves coupling efficiency to a single-mode fiber.

important, however, to assess the performance of any new structure on overall device performance. This section looks at the influence of coupling efficiency variation due to misalignment on the performance of a microring laser. The analysis is based on steady state approximation, and a detailed derivation of the list of relevant equations can be found in [10]. The coupling coefficient of a microring laser structure is analogous to the emission mirror reflectivity of a Fabry–Perot laser, and therefore has significant effect on the differential slope efficiency, intracavity loss, threshold current density, and quality factor of the device.

Fig. 8 shows the percentage of threshold current density $(J_{\rm th})$ deviation, quality factor (Q), and differential slope efficiency (η) against lateral misalignment for conventional (solid line) and proposed (dotted line) design. The threshold current density is given by

$$J_{\rm th} = \frac{ed}{\tau_N}\left[N_T + \frac{1}{a_N \tau_{\rm ph}}\right] \tag{3}$$

where e $(= 1.6 \times 10^{-19})$ is the electron charge, d $(= 0.1$ μm) is the thickness of the active layer, τ_N $(= 1$ ns) is the carrier lifetime, $N_T (= 1.5 \times 10^{18})$ is the transparency carrier density, $a_N (= 1.3 \times 10^{-7})$ is the differential gain coefficient, and $\tau_{\rm ph}$ is the photon lifetime. The quality factor is given by

$$Q = \frac{4\pi^2 R n_{\rm eff}}{\lambda \kappa} \tag{4}$$

where R $(= 20$ μm) is the ring radius, $n_{\rm eff}$ $(= 3.4)$ is the effective refractive index of the guided mode, λ $(= 1.55$ μm) is the operating wavelength, and κ is the coupling coefficient. The internal quantum efficiency is given by

$$\eta_{\rm int} = \frac{\alpha_\kappa}{\alpha_\kappa + \alpha_{\rm abs}} \tag{5}$$

where α_κ is the cavity loss of the optical intensity, and $\alpha_{\rm abs}$ $(= 50\,{\rm cm}^{-1})$ is the absorption/bending loss. In (3)–(5), the photon lifetime and cavity loss are parameters determined by the alignment between the microring and bus waveguide, and are calculated based on standard Fabry–Perot resonator equations (with $R = 1 - \kappa$, where R is the emission mirror reflectivity). Bending loss introduces a constant attenuation to the optical intensity, corresponding to a constant shift in threshold current density and differential slope efficiency. Within the typical range of coupling coefficient (4%-10%), the cavity loss due to photon escaping from the microring cavity is much higher than the internal absorption/bending loss.

The coupler geometry is designed to achieve an identical coupling coefficient for the fundamental mode under perfect alignment. It is clear from the calculations that for conventional design, lateral misalignment results in drastic reduction of coupling coefficient, thereby increasing the deviation of threshold current density and the quality factor of the resonator. The reduction in coupling coefficient due to lateral misalignment increases the Q, and therefore reduces the threshold current density. However, this also causes dramatic deviation of differential slope efficiency from the designated performance. On the other hand, relaxed sensitivity to alignment issue in the proposed multimode bus coupler geometry greatly reduces the influence of lateral misalignment on the laser's slope efficiency.

V. Conclusion

A 3-D mode propagation solver has been implemented to analyze various vertically coupled microring designs within a self-consistent framework. Mode coupling between the two waveguides is addressed by injecting a fundamental mode at the ring and computing the optical output from the bus waveguide. A linear relationship is found between coupling coefficient rolloff and lateral misalignment between the two waveguides for a conventional vertically coupled design employing a single-mode ring and bus waveguide. Although the vertical coupling scheme is more tolerant to fabrication imperfection than the lateral coupling scheme due to the precise control over coupling separation achieved by means of epitaxial growth, this

advantage might well be offset by the lateral misalignment between the ring and bus waveguide introduced during subsequent mask alignments, which is limited to an accuracy of ± 0.3 μm by the current state-of-the-art technology.

The sensitivity of coupling coefficient on lateral misalignment can be readily understood within the framework of coupled-mode theory, which indicates that for two weakly-coupled waveguides, the coupling coefficient is dependent on the mode overlap integral and the length of the coupling region. This has prompted a highly applicable way of relaxing the fabrication tolerance–by employing a mode expanded wide multimode bus waveguide, the sensitivity of the two critical parameters against misalignment can be greatly reduced. Further simulations have confirmed this speculation: for a bus waveguide double the size of the ring, lateral misalignment of 0.3 μm from the optimum coupling point results in a deviation of coupling coefficient of less than 5%. This shows that reproducible vertically coupled microring devices can be realized with existing fabrication technology by employing a wider bus waveguide. The feasibility of applying simple taper architecture to achieve higher order mode filtering and enhanced fiber coupling efficiency is also studied. A double taper with an in-and-out configuration is shown to be effective in discriminating against higher order modes and reducing lateral diffraction, resulting in improved spot-size matching when butt-coupled to a single-mode fiber. The schematic of the proposed design is summarized in Fig. 9. Implications of the proposed structure for device performance are also investigated by comparing the characteristics of a semiconductor microring laser design based on conventional and proposed structure. It is shown that the proposed structure is capable of stabilizing important laser parameters, for instance, differential slope efficiency, against lateral misalignment.

In conclusion, a consistent theoretical analysis of different vertically coupled microring designs has been performed for the first time, highlighting the limitation due to lateral misalignment in achieving a reproducible device. A mode expanded bus waveguide with double taper configuration is proposed, and is subsequently shown to be capable of relaxing the fabrication tolerance.

ACKNOWLEDGMENT

The authors would like to acknowledge discussions with U. Troppenz, M. Hamacher, and H. Heidrich of Heinrich-Hertz-Institute, Germany, for insights into microring fabrication technologies, and D. Gallagher of Photon Design Inc., U.K., for useful discussions on the implementation of the 3-D mode propagation solver, Fimmprop, which was used for the analysis of microring devices in this work.

REFERENCES

[1] M. T. Hill, H. J. S. Dorren, T. Vries, X. J. M. Leijtens, J. H. Besten, B. Smalbrugge, Y. S. Oei, H. Binsma, G. D. Khoe, and M. K. Smit, "A fast low-power optical memory based on coupled micro-ring lasers," *Nature*, vol. 432, pp. 206–209, 2004.

[2] V. R. Almeida, C. A. Barrios, R. R. Panepucci, and M. Lipson, "All-optical control of light on a silicon chip," *Nature*, vol. 431, pp. 1081–1084, 2004.

[3] P. P. Absil, "Microring resonators for wavelength division multiplexing and integrated photonics applications," Ph.D. dissertation, Dept. Elect. Comput. Eng., Univ. Maryland, College Park, MD, 2000.

[4] R. Grover, "Indium phosphide based optical micro-ring resonators," Ph.D. dissertation, Dept. Elect. Comput. Eng., Univ. Maryland, College Park, MD, 2003.

[5] K. Tada and K. Hirose, "A new light modulator using perturbation of synchronism between two coupled guides," *Appl. Phys. Lett.*, vol. 25, no. 10, pp. 561–562, 1974.

[6] M. Cada, R. C. Gauthier, B. E. Paton, and J. Chrostowski, "Nonlinear guided waves coupled nonlinearly in a planar GaAs/GaAlAs multiple quantum well structure," *Appl. Phys. Lett.*, vol. 49, no. 13, pp. 755–757, 1986.

[7] L. C. So and C. A. Lee, "A new integrable optical modulator switch optimized for speed and power consumption," *J. Appl. Phys.*, vol. 66, no. 5, pp. 2200–2205, 1989.

[8] I. B. Djordjevic, R. Varrazza, M. Hill, and S. Yu, "Packet switching performance at 10 Gb/s across a 4×4 optical crosspoint switch matrix," *IEEE Photon. Technol. Lett.*, vol. 16, no. 1, pp. 102–104, Jan. 2004.

[9] M. Sorel, P. J. R. Laybourn, G. Giuliani, and S. Donati, "Unidirectional bistability in semiconductor waveguide ring lasers," *Appl. Phys. Lett.*, vol. 80, pp. 3051–3053, 2002.

[10] M. Sorel, G. Giuliani, A. Scire, R. Miglierina, S. Donati, and P. J. R. Laybourn, "Operating regimes of GaAs-AlGaAs semiconductor ring lasers: experiment and model," *IEEE J. Quantum Electron.*, vol. 39, no. 10, pp. 1187–1195, Oct. 2003.

[11] D. G. Rabus, M. Hamacher, U. Troppenz, and H. Heidrich, "Optical filters based on ring resonators with integrated semiconductor optical amplifiers in GaInAsP-InP," *IEEE J. Sel. Topics Quantum Electron.*, vol. 8, no. 6, pp. 1405–1411, Nov./Dec. 2002.

[12] B. E. Little, S. T. Chu, P. P. Absil, J. V. Hryniewicz, F. G. Johnson, F. Seiferth, D. Gill, V. Van, O. King, and M. Trakalo, "Very high-order microring resonator filters for WDM applications," *IEEE Photon. Technol. Lett.*, vol. 16, no. 10, pp. 2263–2265, Oct. 2004.

[13] Y. Yanagase, S. Suzuki, Y. Kokubun, and S. T. Chu, "Vertical triple series-coupled microring resonator filter for passband flattening and expansion of free spectral range," *Jpn. J. Appl. Phys.*, vol. 41, pp. L141–L143, 2002.

[14] R. Grover, V. Van, T. A. Ibrahim, P. P. Absil, L. C. Calhoun, F. G. Johnson, J. V. Hryniewicz, and P. T. Ho, "Parallel-cascaded semiconductor microring resonators for high-order and wide-FSR filters," *J. Lightw. Technol.*, vol. 20, no. 5, pp. 900–905, May 2002.

[15] C. Manolatou, M. J. Khan, S. Fan, P. R. Villeneuve, H. A. Haus, and J. D. Joannopoulos, "Coupling of modes analysis of resonant channel add-drop filters," *IEEE J. Quantum Electron.*, vol. 35, no. 9, pp. 1322–1331, Sep. 1999.

[16] D. G. Rabus, M. Hamacher, U. Troppenz, and H. Heidrich, "High-Q channel-dropping filters using ring resonators with integrated SOAs," *IEEE Photon. Technol. Lett.*, vol. 14, no. 10, pp. 1442–1444, Oct. 2002.

[17] B. E. Little, S. T. Chu, H. A. Haus, J. Foresi, and P. Laine, "Microring resonator channel dropping filters," *J. Lightw. Technol.*, vol. 15, no. 6, pp. 998–1005, Jun. 1997.

[18] S. T. Chu, B. E. Little, W. Pan, T. Kaneko, S. Sato, and Y. Kokubun, "An eight-channel add-drop filter using vertically coupled microring resonators over AQ cross grid," *IEEE Photon. Technol. Lett.*, vol. 11, no. 6, pp. 691–693, Jun. 1999.

[19] T. A. Ibrahim, W. Cao, Y. Kim, J. Li, J. Goldhar, P. T. Ho, and C. H. Lee, "All-optical switching in a laterally coupled microring resonator by carrier injection," *IEEE Photon. Technol. Lett.*, vol. 15, no. 1, pp. 36–38, Jan. 2003.

[20] K. Djordjev, S. J. Choi, S. J. Choi, and P. D. Dapkus, "Vertically coupled InP microdisk switching devices with electroabsorptive active regions," *IEEE Photon. Technol. Lett.*, vol. 14, no. 8, pp. 1115–1117, Aug. 2002.

[21] P. P. Absil, J. V. Hryniewicz, B. E. Little, P. S. Cho, R. A. Wilson, L. G. Joneckis, and P. T. Ho, "Wavelength conversion in GaAs micro-ring resonators," *Opt. Lett.*, vol. 25, no. 8, pp. 554–556, 2000.

[22] T. A. Ibrahim, K. Amarnath, L. C. Kuo, R. Grover, V. Van, and P. T. Ho, "Photonic logic NOR gate based on two symmetric microring resonators," *Opt. Lett.*, vol. 29, no. 23, pp. 2779–2781, 2004.

[23] K. Djordjev, S. J. Choi, S. J. Choi, and P. D. Dapkus, "High-Q vertically coupled InP microdisk resonators," *IEEE Photon. Technol. Lett.*, vol. 14, no. 3, pp. 331–333, Mar. 2002.

[24] S. J. Choi, K. Djordjev, S. J. Choi, P. D. Dapkus, W. Lin, G. Griffel, R. Menna, and J. Connolly, "Microring resonators vertically coupled to buried heterostructure bus waveguides," *IEEE Photon. Technol. Lett.*, vol. 16, no. 3, pp. 828–830, Mar. 2004.

[25] K. Djordjev, S. J. Choi, S. J. Choi, and P. D. Dapkus, "Study of the effects of the geometry on the performance of vertically coupled InP microdisk resonators," *J. Lightw. Technol.*, vol. 20, no. 8, pp. 1485–1492, Aug. 2002.
[26] P. P. Absil, J. V. Hryniewicz, B. E. Little, F. G. Johnson, K. J. Ritter, and P. T. Ho, "Vertically coupled microring resonators using polymer wafer bonding," *IEEE Photon. Technol. Lett.*, vol. 13, no. 1, pp. 49–51, Jan. 2001.
[27] R. Grover, P. P. Absil, V. Van, J. V. Hryniewicz, B. E. Little, O. King, L. C. Calhoun, F. G. Johnson, and P. T. Ho, "Vertically coupled GaInAsP-InP microring resonators," *Opt. Lett.*, vol. 26, no. 8, pp. 506–508, 2001.
[28] B. E. Little and S. T. Chu, "Estimating surface-roughness loss and output coupling in microdisk resonators," *Opt. Lett.*, vol. 21, no. 17, pp. 1390–1392, 1996.
[29] D. V. Tishinin, P. D. Dapkus, A. E. Bond, I. Kim, C. K. Lin, and J. O. Brien, "Vertical resonant couplers with precise coupling efficiency control fabricated by wafer bonding," *IEEE Photon. Technol. Lett.*, vol. 11, no. 8, pp. 1003–1005, Aug. 1999.
[30] B. Liu, A. Shakouri, P. Abraham, B. G. Kim, A. W. Jackson, and J. E. Bowers, "Fused vertical couplers," *Appl. Phys. Lett.*, vol. 72, no. 21, pp. 2637–2638, 1998.
[31] Fimmwave/FimmProp, Photon Design (Europe) Ltd. [Online]. Available: http:/www.photond.com
[32] D. F. G. Gallagher and T. P. Felici, "Eigenmode expansion methods for simulation of optical propagation in photonics—pros and cons," in *Proc. SPIE-Int. Soc. Opt. Eng. Photonics West,* San Jose, CA, 2003, vol. 4987-10, pp. 69–82.
[33] A. S. Sudbo, "Film mode matching: a versatile numerical method for vector mode field calculations in dielectric waveguides," *Pure Appl. Opt.*, vol. 2, pp. 211–233, 1993.
[34] T. Kato, S. Suzuki, Y. Kokubun, and S. T. Chu, "Coupling-loss reduction of a vertically coupled microring resonator filter by spot-size-matched busline waveguides," *Appl. Opt.*, vol. 41, no. 21, pp. 4394–4399, 2002.

Chyng Wen Tee (S'04) received the B.Eng. degree in electrical and electronic engineering from Nanyang Technological University, Singapore, in 2003. He is currently working toward the Ph.D. degree at the Center for Photonic Systems, University of Cambridge, Cambridge, U.K.

His research interests include semiconductor microring devices, high-brightness laser diodes, and the modal characteristics of vertical cavity surface emitting lasers.

Kevin A. Williams (M'00) received the B.Eng. degree in electrical engineering from the University of Sheffield, Sheffield, U.K., in 1991, and the Ph.D. degree in physics from the University of Bath, Bath, U.K., in 1995.

He was subsequently awarded a Royal Society University research fellowship to study high-speed and high-power laser design at the Department of Electronic Engineering, University of Bristol, Bristol, U.K. In 2001, he joined the University of Cambridge, Cambridge, U.K., where he is a Fellow and Lecturer at Churchill College. He is also a Faculty Affiliate Researcher with Intel Research, Cambridge. He has authored over 100 publications. His research interests are in the area of integrated photonic circuits, including laser, switch, and photonic subsystem design, as well as implementations in switched networks, interconnects, and high capacity transmission.

Richard V. Penty (M'00) received the B.A. degree in engineering and electrical sciences and the Ph.D. degree in nonlinear optical fiber devices from the University of Cambridge, Cambridge, U.K., in 1986 and 1990, respectively.

He was an SERC IT Research Fellow at the University of Cambridge until taking a Lectureship in Physics at the University of Bath, Bath, U.K., in 1990. In 1996, he joined the University of Bristol, Bristol, U.K. as a Lecturer in electrical and electronic engineering, subsequently being promoted to Professor of Photonics. In 2001, he moved to the Cambridge University Engineering Department and was elected to a Fellowship with Sidney Sussex College, University of Cambridge, in 2002. His research interests include optical data communications, MMF systems (digital and analog), high-speed optical communications systems, wavelength conversion and WDM networks, optical amplifiers, optical nonlinearities for switching and routing applications, RF over fiber, and high-power semiconductor lasers.

Dr. Penty is an Honorary Editor of the *IEE Optoelectronics Journal*.

Ian H. White (S'82–M'83–SM'00–F'05) received the B.A and Ph.D. degrees from the University of Cambridge, Cambridge, U.K., in 1980 and 1984, respectively.

He became a Research Fellow and Assistant Lecturer with the University of Cambridge before becoming Professor of Physics at the University of Bath, Bath, U.K., in 1990. In 1996, he moved to the University of Bristol, Bristol, U.K., where he became Head of the Department of Electrical and Electronic Engineering in 1998. He was also Professor of Optical Communications, Head of the Department of Electrical and Electronic Engineering, and Deputy Director of the Center for Communications Research. He returned to the University of Cambridge in October 2001 as the van Eck Professor of Engineering. He is currently Head of the Photonic Research Laboratory, and, in January 2005, was appointed Chair of the School of Technology. He has published in excess of 400 publications and holds 20 patents. His current research interests include high speed communication systems, local area networks using optical links, photonic components, and ultrafast photonics.

Dr. White is currently an Editor of *Optical and Quantum Electronics* and an honorary editor of *Electronics Letters*. He is active in data communications research, contributing to the IEEE802.3aq standard in the area of multimode fiber modeling.